Quantum dot lasers and integrated optoelectronics on silicon platform

Invited Paper

Jun Yang[1], Pallab Bhattacharya[1], Zetian Mi[2], Guoxuan Qin[3], and Zhenqiang Ma[3]

[1]*Department of Electrical Engineering and Computer Science, University of Michigan, Ann Arbor, MI 48015, USA*

[2]*Department of Electrical and Computer Engineering, McGill University, Montreal, Quebec H3A 2A7, Canada*

[3]*Department of Electrical and Computer Engineering, University of Wisconsin, Madison, WI 53706, USA*

Received May 19, 2008

Chip-scale integration of optoelectronic devices such as lasers, waveguides, and modulators on silicon is prevailing as a promising approach to realize future ultrahigh speed optical interconnects. We review recent progress of the direct epitaxy and fabrication of quantum dot (QD) lasers and integrated guided-wave devices on silicon. This approach involves the development of molecular beam epitaxial growth of self-organized QD lasers directly on silicon substrates and their monolithic integration with amorphous silicon waveguides and quantum well electroabsorption modulators. Additionally, we report a preliminary study of long-wavelength (> 1.3 μm) QD lasers grown on silicon and integrated crystalline silicon waveguides using membrane transfer technology.

OCIS codes: 140.5960, 250.3140, 230.5590.

doi: 10.3788/COL20080610.0727.

Optical interconnect systems incorporating chip-scale integration of optical and electronic components on silicon are prevailing as promising substitutes for current microelectronic chips[1,2]. This is because optical interconnects can not only provide higher bandwidth for computing and switching, but also provide advantages such as inherent parallel processing without crosstalk and lower power dissipation. In order to achieve lower cost and good compatibility with mature microelectronics manufacturing, the use of silicon as a fundamental material for the realization of light modulation, guiding, and emission, has been pursued during the past decade[3−5]. Significant progress has been made, despite the challenge that silicon has poor light emission, small linear electro-optic effect, and high waveguide-propagation loss in the wavelength range of $1.3 - 1.55$ μm.

Electro-optical (EO) modulation is crucial for high-speed systems. Unfortunately, the most common EO effects, such as the Pockels effect in $LiNbO_3$ crystal, Kerr effect in polar liquids, and the quantum-confinement Stark effect (QCSE) in III-V compound semiconductors[6], have very low efficiency in silicon. An alternative mechanism of achieving efficient EO modulation in silicon is the free-carrier plasma dispersion effect (FCPDE)[7], which is the linear dependence of refractive index and absorption coefficient on injection carrier density. Based on FCPDE, researchers at Intel recently utilized a metal-oxide-semiconductor (MOS) capacitor to achieve a Mach-Zehnder type modulator with speeds up to 10 Gb/s[8,9]. Another research group extended the above design to achieve a more compact modulator by using a microring resonator[10]. On the other hand, strained silicon exhibits significant electroabsorption modulation. It has been reported that efficient electroabsorption modulation can be achieved by using the electrical-field induced delocalization of the electron wavefunction in strained Si/Ge shallow quantum wells[11]. Recently, enhanced QCSE in strained Si/Ge quantum well was observed[12], which might lead to electroabsorption modulators with efficiency comparable to III-V counterparts.

The propagation loss in silicon arises mainly from the waveguide surface roughness and intrinsic material absorption, where the former is usually dominant[5]. To date, with the development of microfabrication and silicon-on-insulator (SOI) technologies, silicon waveguides exhibit acceptable propagation loss, below 1 dB/cm, in the wavelength range of $1.3 - 1.55$ μm[13]. Another loss in waveguides, especially for high-density integration on a chip, is the radiation loss due to waveguide bending. Using a modified structure with more material compensated in the inner part of the bend, researchers have demonstrated a 90°-bend with 0.7-μm radius and losses less than 1%[14]. Alternatively, low-loss bends with a sub-micrometer radius in photonic-crystal waveguide structures have been demonstrated[15].

As an indirect-bandgap semiconductor, silicon is a poor light emitter. While enhanced electroluminescence has been observed in nano-structured or nanocrystalline silicon[16−18], the efficiency is very small. Recently, a silicon Raman laser using optical pumping was demonstrated[19,20] and this technology has been widely viewed as a milestone in the development of silicon-based lasers. However, in the long run, a silicon laser using electrical injection rather than optical pumping is more desirable for chip-scale integration. An alternate scheme involves a hybrid electrically-driven III-V laser on silicon by using wafer bonding or heteroepitaxial growth. The bonding technique has evolved from simple bonding of the whole III-V laser structure onto a silicon wafer[21] to the more state-of-the-art bonding of III-V gain media onto an evanescent-coupled silicon waveguide cavity[22]. The direct growth of III-V quantum well lasers on silicon has also been extensively investigated by using a variety of buffer layers such as two-dimensional (2D) strained superlattices[23,24], thermal cycle annealing[25],

and graded SiGe buffer layers[26]. However, the reliability of such hybrid electrically-driven devices is still a challenging issue due to incompatibility of III-V semiconductors with silicon. The demonstration of a reliable electrically-pumped silicon laser has been a major and elusive goal in this field, despite the fact that laser-on-chip might not be an ideal architecture due to heat dissipation problems[4]. In this context, we have made significant progresses in realizing quantum dot (QD) lasers directly grown on (001)-oriented silicon substrates. We have also demonstrated monolithic integration of the lasers with silicon and III-V-based waveguides and modulators, all grown and regrown epitaxially on silicon. After these are briefly reviewed, a description of preliminary work on the epitaxy and characterization of long-wavelength QD lasers on silicon and the integration of these devices with crystalline silicon waveguides by using membrane transfer is given.

Now consider the QD lasers directly grown on silicon and their integration with waveguides and modulators. In the context of hybrid III-V lasers on silicon, QD gain media can provide the opportunity to achieve improved performance. Self-organized In(Ga)As/GaAs QDs are formed in the Stranski-Krastanow growth mode[27,28]. Due to the three-dimensional (3D) confinement of carriers and the resulting near-discrete density of states, QD lasers promise significantly improved performance and reliability, compared with quantum well lasers. Near-ideal characteristics, including ultra-low threshold current ($J_{\rm th} \leq 100$ A/cm^2)[29−31], large output power (up to 11.7 W)[32], temperature invariant operation ($T_0 \cong \infty$)[33], large small-signal modulation bandwidth ($f_{-3\,\rm dB} \approx 24.5$ GHz)[34,35], and near-zero chirp and α-parameters[35] have been achieved in $1.0 - 1.55$ μm self-organized QD lasers. In addition, the strain field in and around the dots is much larger than that produced by 2D strained-layer superlattices. Dislocations propagating near and under the dots will experience stronger Peach-Koehler forces and, consequently, such dislocations will be bent more easily. Therefore, in addition to providing the superiority as active media, QDs incorporated in buffer layers can serve as efficient dislocation filters to impede the dislocation propagating from the lattice-mismatched interface to the active region[36].

In the past several years, a detailed study of the monolithic growth, fabrication, and characterization of InGaAs/GaAs QD lasers on silicon, and their on-chip integration with waveguides and modulators has been conducted[36−41]. A novel dislocation reduction technique using self-organized InAs QDs as a dislocation filter was proposed, and its efficiency was analyzed with simulation of quasi-3D strain-dislocation interaction and confirmed with experiments including transmission electron microscopy and photoluminescence. Compared with 2D strained layer superlattices, the QD dislocation filter demonstrates a higher efficiency of blocking both threading dislocations and edge dislocations due to a stronger and anisotropic strain field in and around the nano-sized islands. By incorporating the optimized InAs QD dislocation filter in a buffer layer, we have realized high performance QD lasers on silicon emitting at 1.0 μm with relatively low threshold current ($J_{\rm th} = 900$ A/cm^2), extremely high temperature stability ($T_0 = 278$ K), and reasonably high output power (~ 150 mW)[36−38]. In addition, the ridge-waveguide QD laser on silicon with a dimension of 400×5 (μm) exhibits the small-signal modulation frequency of 5.5 GHz at the injection current of 180 mA, which is comparable to that of QD lasers on GaAs substrates[38]. Some data, which have been previously reported, are shown in Fig. 1 for completeness. It is worthwhile to mention that the measured threshold current of QD lasers on silicon is still much larger than that of identical devices grown on GaAs, which is typically less than 100 A/cm^2. The threshold current is primarily limited by the large dislocation density ($\sim 5 \times 10^7$ cm^{-2}) in the GaAs buffer layer grown directly on Si substrates, which enhances the waveguide loss. It is expected that the use of relatively low ($\leq 1 \times 10^6$ cm^{-2}) defect density buffer layers, such as relaxed and graded SiGe buffer layers[26], in conjunction with InAs QD dislocation filters, may lead to QD lasers on Si with performance characteristics comparable to those grown on GaAs substrates.

High-performance lasing and efficient coupling in an integrated GaAs-based laser-waveguide-modulator system on silicon has also been achieved by utilizing molecular beam epitaxial (MBE) growth, regrowth, and focused-ion-beam (FIB) etching techniques[39,40]. The FIB-etched facets exhibit reflectivity of ~ 0.28, close to the reflectivity of 0.31 for cleaved facets. The QD lasers on both GaAs and silicon with FIB-etched facets exhibit performance comparable to those with cleaved facets. For the monolithically-integrated QD laser and quantum well (QW) absorption modulator, the measured coupling efficiency is more than 20% and the modulation depth is nearly 100% for applied reverse biases of −5 V. The

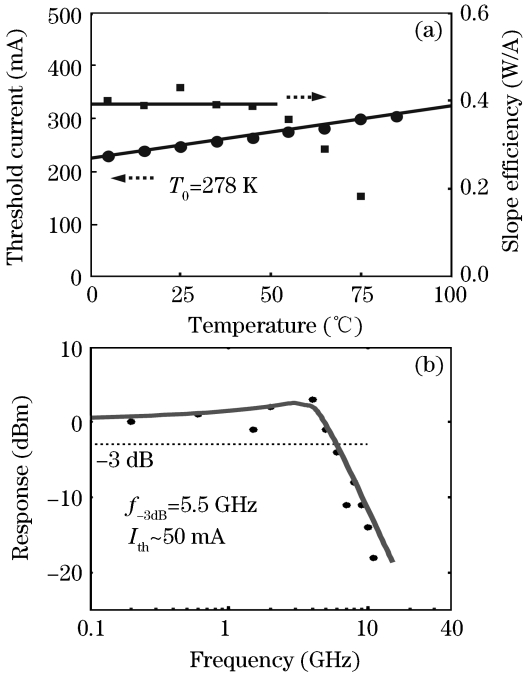

Fig. 1. Characteristics of 1.0-μm QD lasers grown on silicon by MBE with QD dislocation filters. (a) Threshold current and slope efficiency versus temperature under pulsed mode (1% duty cycle of 100 μs); (b) small-signal modulation response.

device performance can be improved by further optimizing regrowth conditions.

An essential component for integrated optoelectronics on Si platform is a low-loss Si waveguide, particularly in the wavelength range of $1.3-1.55$ μm. In this regard, we have investigated groove-coupled QD laser with hydrogenated amorphous Si (a:Si-H) waveguides on silicon[41]. The use of a:Si-H for low-loss Si waveguides offers the additional advantages of low cost, low temperature processing, and other unique characteristics, such as tunable bandgap and refractive index by the hydrogen composition. The waveguide consisting of SiO_x/a:Si-H/SiO_x is formed by plasma-enhanced chemical vapor deposition (PECVD).

The QD lasers on silicon discussed above exhibit lasing wavelengths of ~ 1.0 μm. However, output wavelengths of $1.3-1.55$ μm are desirable for optical communications, silicon photonics, and from the point of view of eye safety. We have investigated the growth and characterization of long-wavelength QD lasers on silicon by incorporating optimized InAs QDs in the active region. GaAs/$Al_{0.7}Ga_{0.3}As$ separate confinement heterostructure QD lasers, as shown in Fig. 2(a), were grown on 4°-misoriented (001) Si substrates utilizing InAs QD dislocation filters that contain ten InAs QD layers separated by 50-nm GaAs barrier layers. The bending of a 60° dislocation induced by the strain field of a QD layer is also illustrated in Fig. 2(a). The laser active region consists of ten InAs QD layers. The p- and n-cladding layers consist of 1.3-μm $Al_{0.7}Ga_{0.3}As$ layers, doped with Be and Si, respectively. The active region QD layers were grown at 510 °C and the rest of the laser heterostructure was grown at $600-620$ °C. Edge-emitting lasers have been fabricated by standard photolithography, wet and dry etching, and contact metallization techniques. Pd/Zn/Pd/Au and Ni/Ge/Au/Ti/Au were deposited by e-beam evaporator as the p- and n-metal contact layers, respectively. The Si substrates were thinned down to $\sim 80-100$ μm to facilitate smooth cleaving along the $\langle 110 \rangle$ direction.

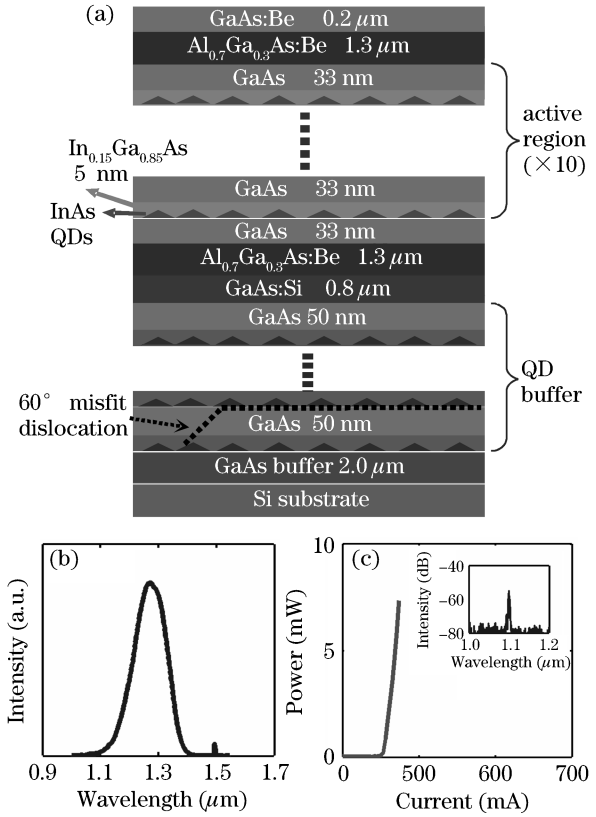

Fig. 2. (a) Schematic of 1.3-μm InAs QD laser heterostructure grown on Si with the incorporation of InAs QDs as dislocation filters. The bending of a 60° dislocation induced by the strain field of a dot layer is illustrated; (b) photoluminescence spectra measured at 300 K (linear scale in y axis); (c) light-current characteristics and the output spectrum (inset) at room temperature.

The photoluminescence spectra exhibit a peak at ~ 1.3 μm, as depicted in Fig. 2(b). However, a preliminary experimental study demonstrates lasing at ~ 1.1 μm with these heterostructures, as shown in Fig. 2(c). This is because lasing takes place from excited states of the QDs, instead of the ground state, due to the existence of relatively high cavity loss. The optimization of high-reflectivity coating may be helpful for achieving ground-state lasing at 1.3 μm. Alternately, we have demonstrated high-performance 1.5-μm metamorphic QD laser on GaAs substrates[29]. With the implementation of this technology onto silicon substrates, as shown in Fig. 3(a), it should be possible to achieve long-wavelength QD lasers on silicon. The photoluminescence peak of these heterostructures is at ~ 1.4 μm (see Fig. 3(b)), which makes 1.3-μm lasing a distinct possibility. This work is on the progress.

As discussed above, a:Si-H waveguides provide low cost benefits and more flexibility in design and fabrication compared with SOI-based waveguides. However,

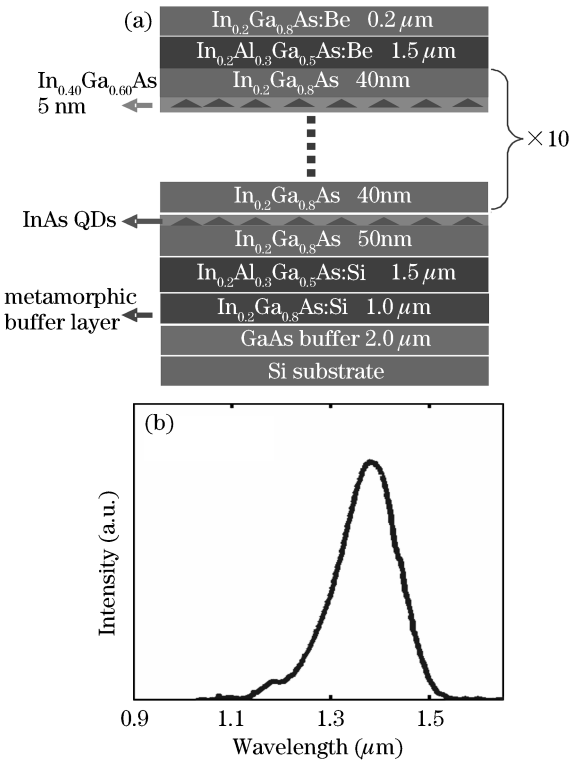

Fig. 3. (a) Schematic of metamorphic long-wavelength InAs QD laser heterostructure grown on Si with the incorporation of InAs QDs as dislocation filters; (b) photoluminescence spectra measured at 300 K (linear scale in y axis).

SOI-based waveguides have lower propagation loss, especially in the wavelength range of $1.3-1.55$ μm, and they are more suitable for electro-optic modulation. Crystalline Si membranes with active devices and circuits can be transferred onto other substrates by a lift-off process[42]. This technology can be extended to achieve low-loss waveguides and electro-optic modulators. Such transferred Si membrane waveguides could have the properties of SOI-based waveguides in addition to providing more flexibility in chip-scale integration.

The integration of a QD light emitting diode (LED) with a transferred Si membrane waveguide has been investigated. The wafer consisting of InGaAs/GaAs QD laser heterostructures was patterned and then dry etched, using Cl_2/Ar inductively coupled plasma (ICP), to delineate the regions where the silicon membrane is to be transferred. Si membranes with a thickness of 0.27 μm were detached from commercial SOI substrates and transferred onto specified regions. PECVD SiO_x as waveguide claddings is deposited before and after the membrane transfer. Next, the ridge waveguide groove-coupled laser-waveguide is fabricated using standard optical photolithography, wet/dry etching, and contact metallization techniques. The wafers are thinned down to ~ 100 μm for cleaving along the $\langle 110 \rangle$ direction. A $\lambda/4$-thick Al_2O_3 thin film as anti-reflection coating is deposited on the waveguide facet by electron beam evaporation. Finally, FIB etching is used to create the coupling groove between the laser and silicon waveguide. The scanning electron microscopy (SEM) image of the whole device is shown in Fig. 4(a). Efficient optical coupling between the LED and transferred Si waveguide has been achieved, as shown in Figs. 4(b) and (c). Work is in progress on the monolithic integration of QD lasers with membrane-transferred Si waveguides on silicon.

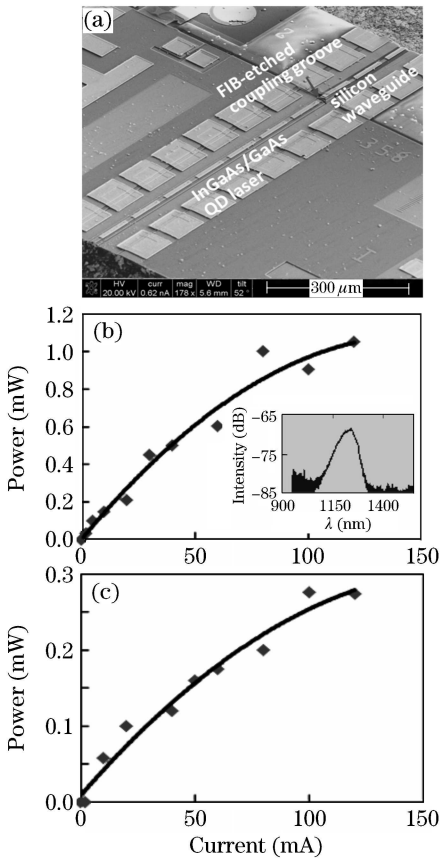

Fig. 4. Monolithic integration of QD LED and crystalline silicon waveguide using silicon membrane transfer technique. (a) SEM image; light-current characteristics for output from (b) the InGaAs QD LED and (c) the coupled silicon waveguide. Inset is the electroluminescence spectrum.

QD lasers and their integration with guided-wave devices have been demonstrated by using a series of techniques including metamorphic MBE growth and regrowth, amorphous-Si waveguide deposition, crystalline Si membrane transfer, and FIB etching. Further improvement in device performance is expected with the use of low-defect density buffer layers on Si, such as relaxed and graded SiGe layers, with implementation of the novel QD dislocation filters. Therefore, the present work may provide a viable approach for future optical interconnect systems on complementary metal oxide semiconductor (CMOS) chips.

This work was supported by the Defense Advanced Research Projects Agency of the United States under Grant No. W911NF-04-1-0429. J. Yang's e-mail address is junyang@umich.edu, and P. Bhattacharya's e-mail address is pkb@eecs.umich.edu.

References

1. J. W. Goodman, F. J. Leonberger, S.-Y. Kung, and R. A. Athale, Proc. IEEE **72,** 850 (1984).
2. D. A. B. Miller, Proc. IEEE **88,** 728 (2000).
3. R. Soref, IEEE J. Sel. Top. Quantum Electron. **12,** 1678 (2006).
4. B. Jalali and S. Fathpour, J. Lightwave Technol. **24,** 4600 (2006).
5. M. Lipson, J. Lightwave Technol. **23,** 4222 (2005).
6. D. A. B. Miller, D. S. Chemla, T. C. Damen, A. C. Gossard, W. Wiegmann, T. H. Wood, and C. A. Burrus, Phys. Rev. Lett. **53,** 2173 (1984).
7. R. A. Soref and B. R. Bennett, IEEE J. Quantum Electron. **23,** 123 (1987).
8. A. Liu, R. Jones, L. Liao, D. Samara-Rubio, D. Rubin, O. Cohen, R. Nicolaescu, and M. Paniccia, Nature **427,** 615 (2004).
9. L. Liao, D. Samara-Rubio, M. Morse, A. Liu, D. Hodge, D. Rubin, U. Keil, and T. Franck, Opt. Express **13,** 3129 (2005).
10. Q. Xu, B. Schmidt, S. Pradhan, and M. Lipson, Nature **435,** 325 (2005).
11. O. Qasaimeh, P. Bhattacharya, and E. T. Croke, IEEE Photon. Technol. Lett. **10,** 807 (1998).
12. Y.-H. Kuo, Y. K. Lee, Y. Ge, S. Ren, J. E. Roth, T. I. Kamins, D. A. B. Miller, and J. S. Harris, Nature **437,** 1334 (2005).
13. K. K. Lee, D. R. Lim, L. C. Kimerling, J. Shin, and F. Cerrina, Opt. Lett. **26,** 1888 (2001).
14. C. Manolatou, S. G. Johnson, S. Fan, P. R. Villeneuve, H. A. Haus, and J. D. Joannopoulos, J. Lightwave Technol. **17,** 1682 (1999).
15. M. Lončar, D. Nedeljković, T. Doll, J. Vučković, A. Scherer, and T. P. Pearsall, Appl. Phys. Lett. **77,** 1937 (2000).
16. W.-H. Chang, A. T. Chou, W. Y. Chen, H. S. Chang, T. M. Hsu, Z. Pei, P. S. Chen, S. W. Lee, L. S. Lai, S. C. Lu, and M.-J. Tsai, Appl. Phys. Lett. **83,** 2958 (2003).

17. R. J. Walters, G. I. Bourianoff, and H. A. Atwater, Nature Mater. **4,** 143 (2005).
18. S. G. Cloutier, P. A. Kossyrev, and J. Xu, Nature Mater. **4,** 887 (2005).
19. O. Boyraz and B. Jalali, Opt. Express **12,** 5269 (2004).
20. H. Rong, R. Jones, A. Liu, O. Cohen, D. Hak, A. Fang, and M. Paniccia, Nature **433,** 725 (2005).
21. H. Wada, H. Sasaki, and T. Kamijoh, Solid-State Electron. **43,** 1655 (1999).
22. A. W. Fang, H. Park, O. Cohen, R. Jones, M. J. Paniccia, and J. E. Bowers, Opt. Express **14,** 9203 (2006).
23. R. Fischer, W. Kopp, H. Morkoç, M. Pion, A. Specht, G. Burkhart, H. Appelman, D. McGougan, and R. Rice, Appl. Phys. Lett. **48,** 1360 (1986).
24. R. D. Dupuis, J. P. van der Ziel, R. A. Logan, J. M. Brown, and C. J. Pinzone, Appl. Phys. Lett. **50,** 407 (1987).
25. T. Egawa, T. Soga, T. Jimbo, and M. Umeno, IEEE J. Quantum Electron. **27,** 1798 (1991).
26. M. E. Groenert, C. W. Leitz, A. J. Pitera, V. Yang, H. Lee, R. J. Ram, and E. A. Fitzgerald, J. Appl. Phys. **93,** 362 (2003).
27. P. R. Berger, K. Chang, P. Bhattacharya, J. Singh, and K. K. Bajai, Appl. Phys. Lett. **53,** 684 (1988).
28. D. Leonard, M. Krishnamurthy, C. M. Reaves, S. P. Denbaars, and P. M. Petroff, Appl. Phys. Lett. **63,** 3203 (1993).
29. Z. Mi, P. Bhattacharya, and J. Yang, Appl. Phys. Lett. **89,** 153109 (2006).
30. G. Park, O. B. Shchekin, S. Csutak, D. L. Huffaker, and D. G. Deppe, Appl. Phys. Lett. **75,** 3267 (1999).
31. P. G. Eliseev, H. Li, T. Liu, T. C. Newell, L. F. Lester, and K. J. Malloy, IEEE J. Sel. Top. Quantum Electron. **7,** 135 (2001).
32. R. L. Sellin, C. Ribbat, D. Bimberg, F. Rinner, H. Konstanrer, M. T. Kelemen, and M. Mikulla, Electron. Lett. **38,** 883 (2002).
33. S. Fathpour, Z. Mi, P. Bhattacharya, A. R. Kovsh, S. S. Mikhrin, I. L. Krestnikov, A. V. Kozhukhov, and N. N. Ledentsov, Appl. Phys. Lett. **85,** 5164 (2004).
34. Z. Mi, P. Bhattacharya, and S. Fathpour, Appl. Phys. Lett. **86,** 153109 (2005).
35. S. Fathpour, Z. Mi, and P. Bhattacharya, J. Phys. D **38,** 2103 (2005).
36. J. Yang, P. Bhattacharya, and Z. Mi, IEEE Trans. Electron Dev. **54,** 2849 (2007).
37. Z. Mi, P. Bhattacharya, J. Yang, and K. P. Pipe, Electron. Lett. **41,** 742 (2005).
38. Z. Mi, J. Yang, P. Bhattacharya, and D. L. Huffaker, Electron. Lett. **42,** 121 (2006).
39. J. Yang, Z. Mi, and P. Bhattacharya, J. Lightwave Technol. **25,** 1826 (2007).
40. J. Yang, P. Bhattacharya, and Z. Wu, IEEE Photon. Technol. Lett. **19,** 747 (2007).
41. J. Yang and P. Bhattacharya, Opt. Express **16,** 5136 (2008).
42. H.-C. Yuan and Z. Ma, Appl. Phys. Lett. **89,** 212105 (2006).